MOLECULAR AND CELLULAR BIOLOGY, Oct. 2008, p. 5924–5936 Vol. 28, No. 19
0270-7306/08/$08.00+0 doi:10.1128/MCB.00560-08

Novel Splicing Factor RBM25 Modulates Bcl-x Pre-mRNA 5′ Splice Site Selection▽

AnYu Zhou,[1,2] Alexander C. Ou,[1] Aeri Cho,[1] Edward J. Benz, Jr.,[1,2,3,4,5] and Shu-Ching Huang[1,2]*

Department of Medical Oncology, Dana-Farber Cancer Institute, Boston, Massachusetts[1]; Department of Medicine, Brigham and Women's Hospital, Boston, Massachusetts[2]; Dana-Farber/Harvard Cancer Center[3] and Department of Pathology, Harvard Medical School,[4] Boston, Massachusetts; and Department of Pediatrics, Children's Hospital, Boston, Massachusetts[5]

Received 7 April 2008/Returned for modification 6 May 2008/Accepted 22 July 2008

RBM25 has been shown to associate with splicing cofactors SRm160/300 and assembled splicing complexes, but little is known about its splicing regulation. Here, we characterize the functional role of RBM25 in alternative pre-mRNA splicing. Increased RBM25 expression correlated with increased apoptosis and specifically affected the expression of Bcl-x isoforms. RBM25 stimulated proapoptotic Bcl-x_S 5′ splice site (5′ ss) selection in a dose-dependent manner, whereas its depletion caused the accumulation of antiapoptotic Bcl-x_L. Furthermore, RBM25 specifically bound to Bcl-x RNA through a CGGGCA sequence located within exon 2. Mutation in this element abolished the ability of RBM25 to enhance Bcl-x_S 5′ ss selection, leading to decreased Bcl-x_S isoform expression. Binding of RBM25 was shown to promote the recruitment of the U1 small nuclear ribonucleoprotein particle (snRNP) to the weak 5′ ss; however, it was not required when a strong consensus 5′ ss was present. In support of a role for RBM25 in modulating the selection of a 5′ ss, we demonstrated that RBM25 associated selectively with the human homolog of yeast U1 snRNP-associated factor hLuc7A. These data suggest a novel mode for Bcl-x_S 5′ ss activation in which binding of RBM25 with exonic element CGGGCA may stabilize the pre-mRNA–U1 snRNP through interactions with hLuc7A.

Alternative splicing is a regulatory mechanism that allows eukaryotes to generate numerous protein isoforms, often with diverse biological functions, from a single gene (2, 26, 49). Pre-mRNA splicing takes place within the spliceosome, which is assembled stepwise by the addition of small nuclear ribonucleoprotein particles (snRNP) and numerous accessory non-snRNP splicing factors (23, 31). The excision of introns and the joining of exons depend on the recognition and usage of 5′ splice sites (5′ ss) and 3′ ss by the splicing machinery (21, 33). The commitment complex forms when the 5′ ss is recognized by U1 snRNA base pairing and stabilized by U1 snRNP while the 3′ ss is recognized by the U2 auxiliary factor (U2AF) through U2 snRNA base pairing with the branch point. Subsequently, the U4/5/6 tri-snRNP is incorporated into the complex and the U1 snRNA base paired at the 5′ ss is replaced by U6 snRNA. These processes result in a fully assembled spliceosome that supports a series of rearrangements via RNA-RNA and RNA-protein interactions and activates the catalytic steps of cleavage, exon joining, and intron release (2, 26).

However, the splice site signals that define the 5′ ss and 3′ ss are often degenerate. How and when they are used are believed to be modulated by a combinational interplay of positive (splicing enhancers) and negative (splicing silencers) *cis* elements and *trans*-acting factors (2, 26), forming the basis of alternative splicing. The splicing regulatory (SR) proteins (18, 41) and the heterogeneous nuclear ribonucleoproteins (hnRNPs) (11, 46) bind with specificity to pre-mRNA (20). The SR proteins generally bind to enhancer elements through the RNA-binding domain and activate splicing at the nearby sites by recruiting spliceosomal components via protein-protein interactions mediated by the arginine-serine-rich (RS) domain (18, 41). The hnRNPs mostly bind to splicing silencers and inhibit the use of the nearby splice site, either by antagonizing positive regulators or by recruiting factors that impede the splicing machinery (11, 57).

A number of other protein families that consist of one or more RNA recognition motifs (RRM) (27) and confer tighter RNA-binding specificity have become visible as splicing regulators, e.g., PurH (39), Sam68 (35), TIA-1 (10), SAP155 (28), and Fox-2 (54). Some are composed of arginine-aspartic acid (RD), arginine-glutamic acid (RE), arginine-glycine-rich motifs, and/or other domains (19, 44, 50) that can mediate interactions between protein and RNA or protein molecules. By associating with different types of protein domains, the RRM domain can modulate its RNA-binding affinity and specificity in alternative splicing (19, 44, 50).

Even though splicing regulation occurs at every step throughout the assembly pathway, many factors primarily affect the efficiency of commitment complex formation (3, 47). Binding of SF2/ASF to an exonic enhancer of rat β-tropomyosin pre-mRNA can stimulate U2AF or U2 binding to a weak 3′ ss and U1 snRNP binding to a 5′ ss (43). Fox proteins interact with the upstream UGCAUG elements in a manner that blocks $U2AF^{65}$ binding to the 3′ ss upstream of exon 4 and prevents exon inclusion in calcitonin/CGRP pre-mRNA (55). Interestingly, human homologs of yeast U1 snRNP-associated proteins, TIA-1 and hLuc7A, have emerged as important players that affect splice site selection. TIA-1 promotes U1 snRNP binding to a weak 5′ ss, followed by uridine-rich sequences

* Corresponding author. Mailing address: Department of Medical Oncology, Dana-Farber Cancer Institute, 44 Binney Street, Boston, MA 02115. Phone: (617) 632-6965. Fax: (617) 632-2662. E-mail: shu-ching_huang@dfci.harvard.edu.

▽ Published ahead of print on 28 July 2008.

through the glutamine-rich domain of TIA-1 and the U1-specific protein U1-C (14). Interaction of yeast yLuc7p with the upstream exon stabilizes the pre-mRNA–U1 snRNP interaction (15). Similarly, human hLuc7A affects 5′ ss selection possibly via the formation of a network of protein-RNA interactions that stabilize pre-mRNA–U1 snRNP interaction and thus formation of the commitment complex (36).

Alternative splicing is often tightly regulated in a cell type- or developmental-stage-specific manner. Splice site selection must therefore depend not only on the *cis* element's identity but also on the amount and/or activities of cellular splicing factors (25, 29). We have shown earlier that expression of RRM-containing splicing factors is regulated during erythroid differentiation (53, 54); RBM25 expression was downregulated during differentiation. RBM25 belongs to a family of RNA-binding proteins whose members share the RE/RD-rich (ER) central region and C-terminal proline-tryptophan-isoleucine (PWI) motif (16). RBM25 localizes to the nuclear speckles and associates with multiple splicing components such as splicing cofactors SRm160/300, U snRNAs, assembled splicing complexes, and spliced mRNAs (16). The characterization of RBM25 strongly suggests that it functions in pre-mRNA processing. However, immunodepletion of RBM25 did not alter the splicing activity of several tested pre-mRNAs, including dsx, Ftz, and Msl-2 (16), suggesting that RBM25 is not a general splicing factor.

Here, we report that RBM25 associates with a U1 snRNP-associated factor, hLuc7A (36), and activates proapoptotic Bcl-x_S 5′ ss via its interaction with the exonic splicing enhancer, CGGGCA. Furthermore, the intracellular RBM25 levels affect the ratio of proapoptotic Bcl-x_S to antiapoptotic Bcl-x_L mRNA and correlate with apoptotic cell death. These data suggest a novel mechanism of Bcl-x_S 5′ ss activation in which binding of RBM25 to exonic element CGGGCA may stabilize the pre-mRNA–U1 snRNP through interaction with hLuc7A. Thus, RBM25 is one of the RNA-binding regulators that direct the alternative splicing of apoptotic factors.

MATERIALS AND METHODS

Plasmid constructs. All DNA constructs were made by using standard cloning procedures and confirmed by sequencing. RBM25 (GenBank accession number NP_067062.1) was amplified from human skeletal muscle cDNA (Origene) with primers 5′-TCTTTTCCACCTCATTTGAATCGC-3′ and 5′-CTTCACAAGAC CAATTTTCTTGGCTTC-3′ and cloned into the expressing vector pCDNA3.1-HA (Invitrogen) to generate pCDNA3.1-HA-RBM25. Full-length RBM25 (amino acids [aa] 1 to 843) and its individual RRM (aa 11 to 284), ER (aa 285 to 644), and PWI (aa 645 to 843) domains were cloned into pEGFP-C2 to generate RBM25-FL/EGFP (where EGFP is enhanced green fluorescent protein), RBM25-RRM/EGFP, RBM25-ER/EGFP, and RBM25-PWI/EGFP, respectively. Full-length RBM25 and its CTD (C-terminal domain; aa 641 to 830) were cloned into pGEX-6p1 to generate RBM25-FL/GST and RBM25-CTD/GST. Full-length RBM25 was cloned into the pcDNA3.1-T7 tag vector (Novagen) to generate RBM25/T7. RBM25 shRNA plasmids with the targeted nucleotide sequences GCTCCAGAGGATGGAACAAGAGGCTGAGA for sh81, CTCCATCTGTT TCCTCTGCCAGTGGCAAT for sh82, CCACTGTGTCTATGGTTGGAAAG CATTTG for sh83, and CTTCGGATTCTGTGAGTACAAGGAGCCAG for sh84 were purchased from Origene.

The Bcl-x minigene was a gift from C. E. Chalfant (Virginia Commonwealth University, Richmond). The Bcl-x exon 2 mutation and Bcl-x_S 5′ ss mutation minigenes were constructed with a QuikChange II XL site-directed mutagenesis kit (Stratagene).

pCGT7-hLuc7A (GenBank accession number NM_01624.3) was kindly provided by O. Puig (European Molecular Biology Laboratory, Germany). The full length (aa 1 to 442), N half (aa 1 to 224), and C half (aa 225 to 442) of hLuc7A were subcloned into pGEX-6p1 (Amersham Biosciences) to produce hLuc7A-FL/GST, hLuc7A-N/GST, and hLuc7A-C/GST, respectively. The E1A minigene (pCEP4-E1A) was a gift from W. Y. Tarn (Institute of Biomedical Sciences, Academia Sinica, Taipei, Taiwan).

Cell culture, transfection, and apoptosis induction. HeLa and HEK293 cells were obtained from the American Type Culture Collection and cultured in Dulbecco modified Eagle medium supplemented with 0.1 mM nonessential amino acids, 1.0 mM sodium pyruvate, 10% fetal calf serum (Invitrogen), and penicillin/streptomycin (5,000 U/ml; Invitrogen). For transcription inhibition, 5,6-dichloro-1-β-D-ribofuranosylbenzimidazole (DRB) was added at 100 μM and the culture was incubated for 2 h at 37°C prior to fixation and immunolabeling. Cells were transfected with Lipofectamine (Invitrogen) according to the manufacturer's instructions. Apoptosis was induced by addition of 500 nM staurosporine (Sigma) in medium and incubation for 0, 24, or 48 h.

RT-PCR analyses. Semiquantitative reverse transcription (RT)-PCR analysis of splicing products was performed as described previously (53). RNAs were reverse transcribed with pcDNA3.1/BGH primer for Bcl-x minigenes. Amplification of spliced products was performed with a pcDNA 3.1 sequence (5′-CTG ATCAGCGGTTTAAACTTA-3′) and a primer specific to Bcl-x exon 2 (5′-GGA GCT GGT GGT TGA CTT TCT-3′). For each construct, two transfections were performed in each experiment. Each experiment was repeated three times, and standard deviations (SDs) were determined.

For E1A splicing analyses, RT was performed with primer P1 (5′-GGTCTT GCAGGCTCCGGTTCTGGC) and PCR was performed with primers P2 (5′-GCAAGCTTGAGTGCCAGCGAGTAG) and P3 (5′-CTCAGGCTCAGGTT CAGACACAGG).

Primer sets flanking exon 2 of Mcl1 (RT, 5′-ATTAGATATGCCAAACCAG C-3′; PCR, 5′-TGGAGATTATCTCTCGGTACCT-3′ and 5′-CAACACCTGC AAAAGCCAGCA-3′), exon 6 of caspase 3 (RT, 5′-GTTGCCACCTTTCGGT TAAC-3′; PCR, 5′-TCAGAGGGGATCGTTGTAGAAG-3′ and 5′-ATGTGC ATAAATTCAAGCTTGTCG-3′), exon 2 of Bcl-x (RT, 5′-AGGGTTGCACC AATCAGGTAG-3′; PCR, 5′-ATGTCTCAGAGCAACCGGGAGCTG-3′ and 5′-TCATTTCCGACTGAAGAGTGAGCC-3′), and exon 6 of Fas (RT, 5′-AG GATTTAAAGTTGGAGAT-3′; PCR, 5′-ATGGAATCATCAAGGAATGCA CA-3′ and 5′-GAGAACCTTGGTTTTCCTTTCTG-3′) were used to analyze the endogenous splicing patterns of its respective genes.

Indirect immunofluorescence and imaging. HeLa and HEK293 cells were transfected with either the pEGFP vector or RBM25/EGFP constructs and subjected to immunofluorescence staining with anti-SC35 antibody (Ab), anti-active caspase 3 Ab (Sigma), or anti-T7 Tag Ab (Novagen) as described previously (54). Endogenous RBM25 was stained with an anti-RBM25 Ab. All samples were counterstained with 4′,6′-diamidino-2-phenylindole (DAPI). The samples were viewed with a Zeiss Axiovert 200M inverted microscope (Zeiss, Inc.). The images were collected with SlideBook4 software and processed with Photoshop software (Adobe Systems, Inc.).

RIP. RNA immunoprecipitation (RIP) was performed as described previously (32). Briefly, 2×10^8 HeLa cells were cross-linked with formaldehyde and resuspended in FA lysis buffer (50 mM HEPES-KOH, 140 mM NaCl, 1 mM EDTA, 0.1% sodium deoxycholate, 1.0% Triton X-100, pH 7.5) containing protease inhibitors and RNase inhibitors. Lysates were sonicated and treated with DNase. Soluble extracts were incubated with anti-RBM25 or rabbit immunoglobulin G (IgG), washed with lysis buffer, digested with RNase-free DNase (Roche), and finally treated with proteinase K. The RNA segments retrieved and the input saved were analyzed by RT-PCR for the presence of Bcl-x or Mcl1 with a random primer for RT. PCR was performed with primer sets Bcl-x1-S (5′-A TGTCTCAGAGCAACCGGGAGCTG-3′) and Bcl-x1-As (5′-CTGTTGGGGA TCTCTGACCAGA-3′) for Bcl-x and hMcl1-Ex2-S (5′-AAGACGATGTGAA ATCGTTGTCTC-3′) and hMcl1-Intr2-As (5′-TCCTTCATTCTACTTCCACT CCA-3′) for Mcl1.

In vitro assays. Gel mobility shift assays were performed as described previously (24), with modification. The biotinylated wild-type (WT) UACCGGCGG GCAUUCAGUGA and mutated UACCGGUUAGAGUUCAGUGA RNA substrates were synthesized by Invitrogen. Binding of biotinylated RNA to RBM25 was achieved by incubating 0.2 nM RNA and variable amounts of protein for 30 min at 4°C in 20 μl of binding buffer (10 mM Tris-HCl, 10 mM HEPES, 100 mM NaCl, 0.1% Triton X-100, 2 mM $MgCl_2$, 1.5 mM dithiothreitol [DTT] [pH 7.5], 7% glycerol). For competition assays, a molar excess of unlabeled competitor RNAs at various levels was added to the preincubation reaction mixture. Samples were fractionated in a native 5% polyacrylamide gel, transferred to Hybond-N+ nylon membrane (Amersham Biosciences), and detected with a LightShift chemiluminescent electrophoretic mobility shift assay kit (Pierce) by following the manufacturer's protocol. RBM25 proteins were purified from nuclear extracts of RBM25/T7-transfected HeLa cells with a T7 · Tag

affinity purification kit (Novagen). Psoralen cross-linking reactions were carried out as described previously (56), with transcripts spanning the region from 92 nucleotides (nt) upstream to 33 nt downstream of the WT, mu4, or consensus Bcl-x_S 5′ ss in the presence or absence of 300 ng purified RBM25. The cross-linked RNAs were analyzed on 5% polyacrylamide gels containing 8.3 M urea.

Co-IP and immunoblotting. Coimmunoprecipitation (co-IP) of RBM25 and hLuc7A was performed with HeLa cell nuclear extracts prepared as described previously (12). Nuclear extracts were diluted in co-IP buffer (30 mM Tris-HCl, 100 mM NaCl, 10 mM $MgCl_2$, 1 mM DTT, 0.5% Triton X-100 [pH 7.5], protease inhibitors) and precleared with rabbit IgG. Subsequently, the supernatant was immunoprecipitated with preimmune rabbit IgG or anti-RBM25 Ab. The immunoprecipitated samples were treated with RNase and examined for the presence of RBM25 with an anti-RBM25 Ab or for the presence of hLuc7A with an anti-Luc7A Ab (Novus).

An anti-RBM25 polyclonal Ab was raised against RBM25-CTD/GST fusion proteins. RBM25 proteins were detected with an antihemagglutinin (anti-HA) Ab (Roche Diagnostics) for HA-tagged RBM25 or with an anti-RBM25 Ab for endogenous RBM25 with the ECL detection kit (Amersham Pharmacia). An anti-β-actin Ab (Sigma) served as a loading control.

GST pull-down assays. Glutathione *S*-transferase (GST) alone or Luc7A/GST fusion proteins were affinity purified via coupling to glutathione-Sepharose beads (GE Healthcare) according to the manufacturer's procedure. Equal amounts of GST fusion proteins were incubated with 500 μg of HeLa cell nuclear extracts in the binding buffer (30 mM Tris-HCl, 100 mM NaCl, 10 mM $MgCl_2$, 1 mM DTT, 0.5% Triton X-100 [pH 7.5], protease inhibitors). The presence of RBM25 bound to Luc7A was detected by Western blotting with an anti-RBM25 Ab.

Annexin V staining. Transfected cells grown on 35-mm plates were harvested and processed for annexin V staining or for Western blot analysis. For annexin V staining, cells were washed in phosphate-buffered saline and stained with annexin V-phycoerythrin (BD Biosciences) according to the manufacturer's instructions. GFP-positive cells were then analyzed with a FACScalibur flow cytometer (Becton Dickinson).

RESULTS

RBM25 localizes to splicing factor-rich nuclear speckles via the ER domain. RBM25 consists of a proline-rich region and an RRM domain at the amino-terminal end, an RE/RD-rich (ER) domain in the central region, and a PWI domain at the carboxyl-terminal end (Fig. 1A). RBM25 is known to localize to nuclear speckles (16). Our Ab against the C-terminal domain of RBM25 confirmed that endogenous RBM25 localized predominantly in the nuclear speckles as a punctate structure (Fig. 1B, −DRB, RBM25). As previously reported, SC35 also localized to the nuclear speckles (Fig. 1B, −DRB, SC35). Superimposition of RBM25 and SC35 revealed that both proteins are intensely colocalized in the same region (Fig. 1B, −DRB, SC35 + RBM25). Upon treatment with DRB, an inhibitor of RNA polymerase II-dependent transcription, both proteins relocated to enlarged and more round nuclear speckles (Fig. 1B, +DRB, SC35, and RBM25). Speckles function as storage compartments that can supply splicing factors to active transcription sites. Splicing factors are recruited from speckles to sites of transcription (30); conversely, splicing factors accumulate in enlarged and rounded speckles when transcription is inhibited (30, 48). The colocalization and co-redistribution of RBM25 and SC35 suggest that RBM25 is organized in a pattern very similar to that of other splicing factors during states of transcriptional activity and quiescence.

To further characterize the domain in RBM25 responsible for speckle localization, we expressed full-length RBM25, as well as its individual RRM, ER, and PWI domains, fused with EGFP in HeLa cells and analyzed its localization relative to splicing factor SC35. EGFP was detected throughout the cell when transfected with the vector alone (Fig. 1C, GFP vector, GFP). The localization of full-length RBM25 was similar to that of endogenous RBM25; it colocalized with SC35 in nuclear speckles (Fig. 1C, RBM25/FL, RBM25 + SC35). A different labeling pattern was observed for the RRM- and PWI-EGFP fusions. Both domains diffusely localized throughout the nucleus without any apparent accumulation on the speckles (Fig. 1C, RBM25/RRM and RBM25/PWI, GFP). The ER domain produced a speckle pattern within the nucleus that coincided with that of SC35 (Fig. 1C, RBM25/ER, RBM25 + SC35). Nuclear speckle localization of the ER domain was not cell type specific, as similar localization was seen in transfected murine erythroleukemia cells (data not shown). Thus, the ER domain of RBM25 is responsible for targeting RBM25 to the nuclear speckle.

RBM25 overexpression correlates with increased apoptotic cell death. Although transient transfection of RBM25 localized to the nuclear speckles, our attempts to achieve stable RBM25 expression lines failed. These cells began to undergo apoptosis between 48 and 72 h after RBM25 introduction.

To gain more insight into the nature of these events, we first transfected HEK293 cells with EGFP or RBM25/EGFP and subsequently determined the extent of cell death by annexin V binding, cleavage of caspase 3, and nuclear fragmentation assays. Cells harvested 48 h after transfection showed a threefold increase in annexin V-positive cells in RBM25/EGFP-transfected cells compared with that of EGFP cells (Fig. 2A). Increased expression of RBM25 also significantly increased the percentage of activated-caspase 3-stained, GFP-positive populations (Fig. 2B). Furthermore, a significant fraction of RBM25-overexpressing cells displayed typical nuclear fragmentation associated with apoptotic cell death (Fig. 2C). These results suggest that an elevation in RBM25 expression caused an increase in apoptotic cell death, indicating that a correlation exists between RBM25 activity and induction of apoptosis.

We then documented the time course of this effect as revealed by nuclear fragmentation in approximately 500 RBM25/GFP-expreesing cells at 24, 48, and 72 h after transfection. At 24 h, different degrees of RBM25/GFP expression, as judged by the intensity/brightness of green fluorescence, were observed. In cells exhibiting "average" brightness, which applied to approximately 95% of the cells, RBM25/GFP localized to nuclear speckles. Of interest, nuclear fragmentation occurred in ~5% of the cells; these cells exhibited above-average brightness. The cells in Fig. 1B and C expressed an average intensity of RBM25/GFP and nuclear speckle localization and are thus indicative of the vast majority of the cells observed.

At 48 h posttransfection, RBM25/GFP accumulated in large aggregates in the nuclei of approximately 25% of the expressing cells (Fig. 2D, RBM25-GFP, GFP, arrow). These cells displayed various degrees of nuclear fragmentation (Fig. 2D, RBM25-GFP, DAPI, arrow). The number of cells exhibiting nuclear fragmentation increased to 50% as transfected cells proceeded to 72 h. We were unable to select stable lines carrying RBM25 due to cell death caused by its overexpression.

We further analyzed the average exogenously expressed RBM25 in the transfected cells by Western blot analysis with an anti-RBM25 Ab. At 48 h posttransfection, an ~1.3- to 1.5-fold increase in RBM25/GFP expression (Fig. 2E, RBM25-GFP, RBM25-GFP) over that of endogenous RBM25 (Fig. 2E, RBM25-GFP, RBM25) was detected in total cell lysates. Tak-

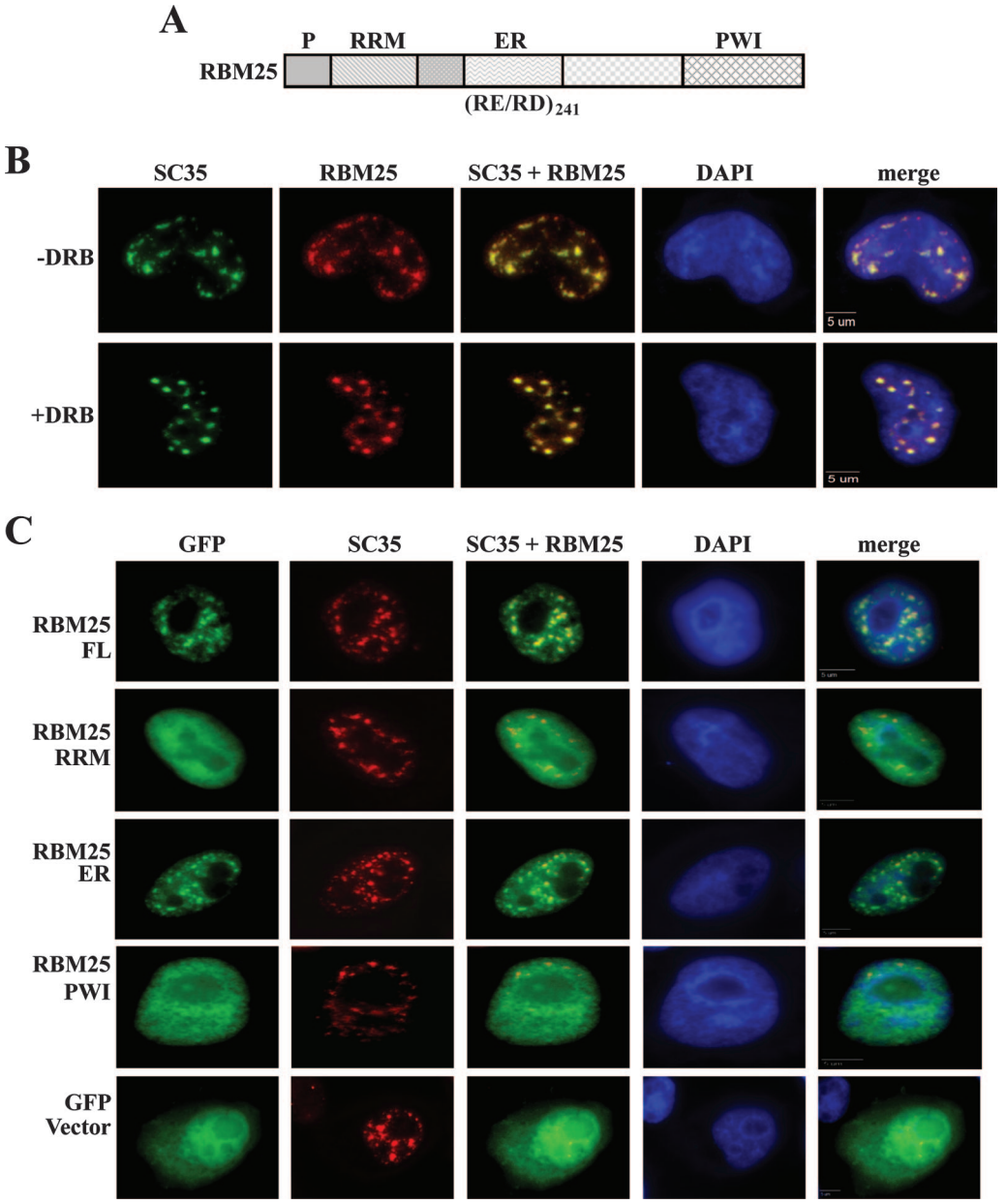

FIG. 1. RBM25 localizes to splicing factor-rich nuclear speckles through the ER domain. (A) Schematic diagram of the structural organization of RBM25. RBM25 is composed of a proline-rich region (P) and an RRM at the amino-terminal end, an RE/RD-rich (ER) domain at the central region, and a PWI domain at the carboxyl-terminal end. (B) Nuclear speckle localization of RBM25 in response to transcriptional inhibition by DRB. HeLa cells were grown in the absence or presence of 100 μM DRB for 2 h at 37°C, processed for immunofluorescence analysis with Abs directed against RBM25 or SC35, and revealed with an Alexa- or fluorescein isothiocyanate-conjugated secondary Ab, respectively. DAPI stains DNA. Bars, 5 μm. (C) The ER domain is critical for RBM25 localization to nuclear speckles. The full length (FL) or the RRM, ER, or PWI domain of RBM25, fused with pEGFP, was transfected into HeLa cells. The expressed EGFP fusion proteins were analyzed for localization relative to splicing factor SC35. Cells were fixed and stained with anti-SC35 Ab and DAPI. Bars, 5 μm.

ing into account the facts that every cell did not express equal amounts of RBM25/GFP and that only approximately 80% transfection efficiency was achieved, we estimate that the average RBM25/GFP expression is approximately 1.6- to 2.0-fold over that of endogenous RBM25. This amount of overexpression is sufficient to induce apoptosis.

Subcellular localization and expression of RBM25 during induced apoptosis. To examine whether RBM25 expression and localization changed during apoptosis, HEK293 cells were treated with staurosporine for 0, 24, and 48 h and analyzed. Nuclear speckle localization of RBM25 was observed in untreated cells (Fig. 3A, 0 h, RBM25). At 24 h, in the majority of the cells, RBM25 accumulated in large aggregates in the nucleus; these aggregates appeared to reside in subnuclear locations containing less condensed DNAs. Nuclear fragmentation was observed in a small population of cells. As apoptosis pro-

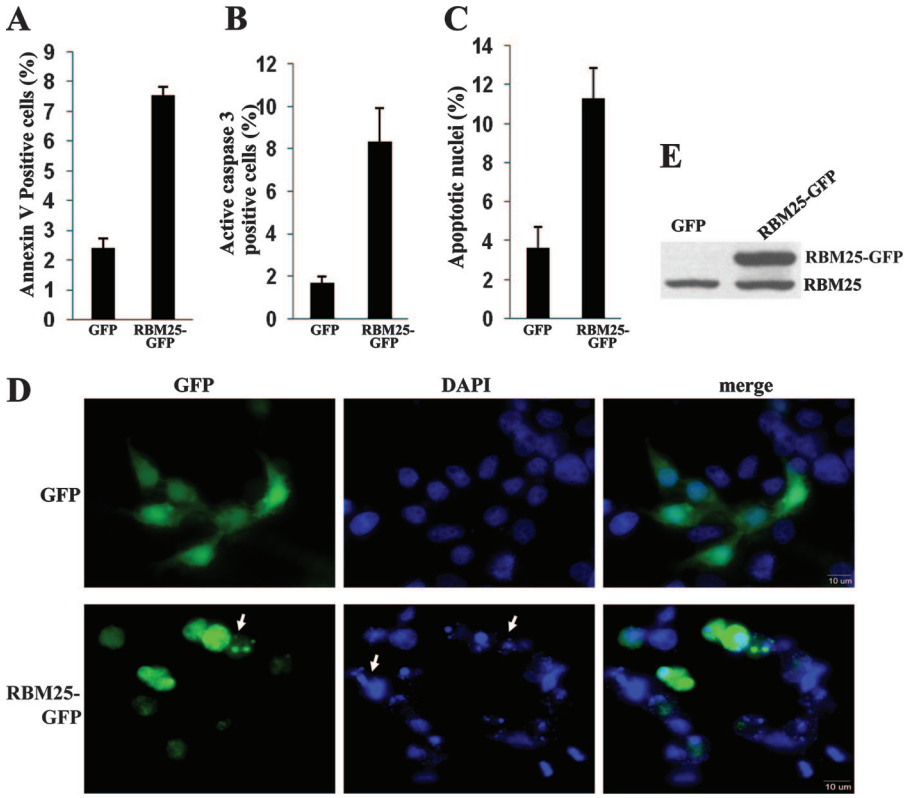

FIG. 2. Increased RBM25 expression correlates with induction of apoptosis. HEK293 cells were transfected with EGFP or RBM25/EGFP. The development of apoptosis was assessed by annexin V binding of GFP-positive cells, by activated (cleaved) caspase 3 immunofluorescent staining, and by DAPI staining scores of nuclear fragmentation. (A) Percentage of cells positive for annexin V-phycoerythrin in the GFP-positive populations. Annexin V staining was performed 48 h after transfection. Data are the mean ± SD of three separate experiments. (B) Percentage of cells positive for activated caspase 3 in the GFP-positive population detected by immunofluorescent staining with anti-caspase 3 Ab 48 h after transfection. At least 500 GFP-positive cells for each sample were counted in each experiment. Data are the mean ± SD of three independent experiments. (C) Percentage of cells positive for nuclear fragmentation in the GFP-positive population. Cells were fixed 48 h after transfection, stained with DAPI, and analyzed for DAPI-stained nuclear fragmentation. Data were obtained by analyzing at least 300 GFP-positive cells for each sample and represent the mean ± SD of three separate experiments. (D) Nuclear fragmentation in cells 72 h after transfection as visualized by DAPI staining. The arrows indicate typical apoptotic cells with RBM25 accumulation or fragmented nuclei. Bars, 10 μm. (E) Western blot analysis of exogenously expressed RBM25-GFP protein at 48 h posttransfection in HEK293 cells. Thirty-five micrograms of cell lysate was fractionated by 8% sodium dodecyl sulfate-polyacrylamide gel electrophoresis and detected with an anti-RBM25 Ab.

ceeded to 48 h, RBM25 accumulated in the subnuclear compartment with less condensed DNAs in some cells (Fig. 3A, 48 h, RBM25, DAPI, merge, arrow) and a diminished RBM25 immunostaining signal was present in the majority of the cells with nuclear fragmentation (Fig. 3A, 48 h, RBM25, DAPI, merge, arrowhead).

We then examined whether RBM25 expression changed during the process. Equal amounts of cell lysates from both induced and uninduced cells were blotted with an anti-RBM25 Ab. An almost equally expressed 120-kDa band was detected in all samples (Fig. 3B, RBM25, lanes 0, 24, 48, and 72). An additional higher-molecular-weight band was also detected in time zero and uninduced 24-h lysates (Fig. 3B, RBM25, lanes 0 and −24). These results suggest that RBM25 expression changes could result from either posttranslational modification or expression of different isoforms. Western blot analysis also clearly demonstrated that the disappearance of RBM25 at 48 h in cells in which apoptosis had been induced was not due to protein degradation because RBM25 remained as intact and abundant in Western blot assays of apoptotic cells as it appeared at time zero (Fig. 3B, lanes 0 and 48). These results imply a possible conformational change occurring in RBM25 that modifies the antigenic epitope recognized by the anti-RBM25 Ab.

RBM25 overexpression affects Bcl-x isoform expression. The observations that RBM25 colocalized with splicing factors in the nuclear speckles and that its overexpression resulted in increased apoptotic cell death suggest a possible role for RBM25 in splicing regulation involved in the apoptotic pathway. This prompted us to search for targets of RBM25 with a focus on apoptotic factors. A large number of these factors are regulated via alternative splicing, a process that allows for the production of discrete protein isoforms with distinct apoptotic functions (42).

We analyzed a panel of apoptotic factors, Mcl1 (1), caspase-3 (22), Bcl-x (4), and Fas (13), for the expression of their isoforms in response to RBM25 overexpression (Fig. 4A). Expression of RBM25 was validated by Western blotting with anti-HA Abs (Fig. 4A, anti-HA). Among the tested factors, increased Bcl-x_S and reduced Bcl-x_L were noted in the pres-

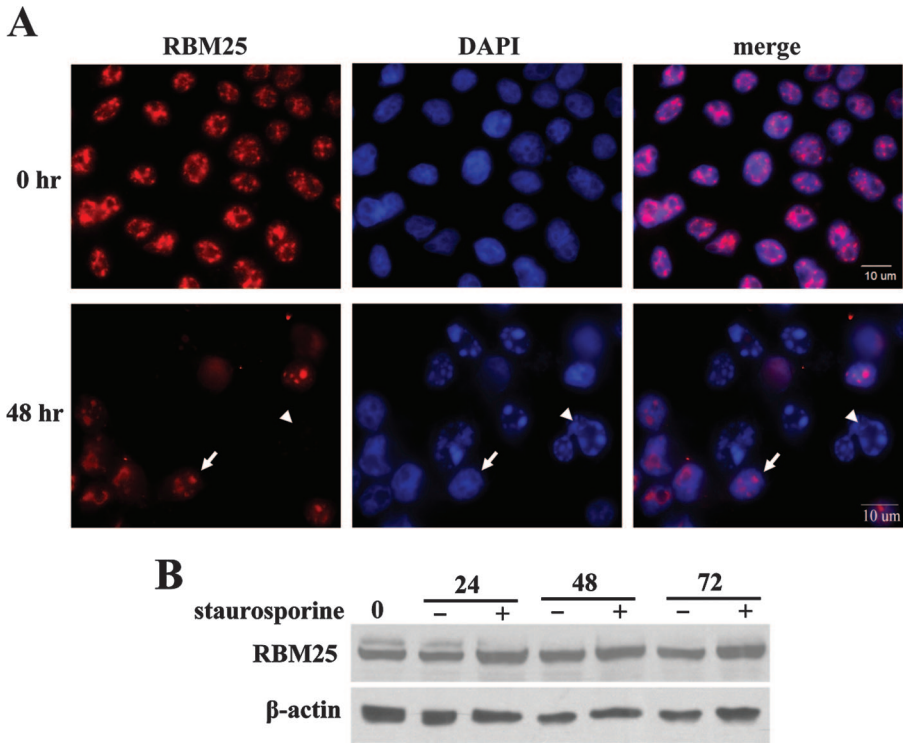

FIG. 3. Expression and localization of RBM25 during staurosporine-stimulated apoptosis in HEK293 cells. (A) Cellular localization of RBM25 at the indicated time points after staurosporine stimulation. HEK293 cells were mock treated or treated with 500 nM staurosporine and stained with anti-RBM25 Ab and DAPI. Bars, 10 μm. (B) Western blot analysis of RBM25 protein levels in HEK293 cells at the indicated time points after either mock treatment (−) or treatment with staurosporine (+). Thirty-five micrograms of cell lysate was fractionated by 8% sodium dodecyl sulfate-polyacrylamide gel electrophoresis and detected with an anti-RBM25 Ab. β-Actin served as a loading control.

ence of RBM25 (Fig. 4A, Bcl-x), implying that RMB25 may regulate Bcl-x alternative splicing. Bcl-x pre-mRNA uses an alternative 5′ ss to produce the antiapoptotic Bcl-x_L or the proapoptotic Bcl-x_S isoform. RBM25 exerted its effect on more

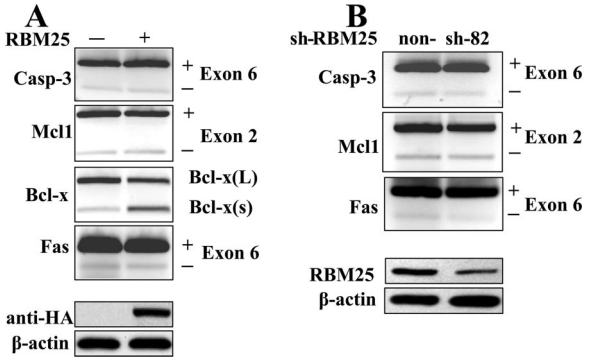

FIG. 4. Effect of RBM25 on alternative splicing of selected apoptotic factors. pCDNA3.1-HA-RBM25-transfected or RBM25 shRNA-depleted HeLa cells were analyzed for alternative splicing patterns of exon 6 of caspase 3, exon 2 of Mcl1, Bcl-x_S and Bcl-x_L of Bcl-x, and exon 6 of Fas by RT-PCR with the respective primer sets. (A) RNA isolated from cells transfected with pCDNA3.1-HA-RBM25 were analyzed for splicing patterns of the indicated genes. Expression of HA-RBM25 was detected in a Western blot assay with an anti-HA Ab. β-Actin served as a loading control. (B) RNA isolated from RBM25 sh-82-depleted cells were analyzed for splicing patterns of the indicated genes. Expression of RBM25 was detected in a Western blot assay with an anti-RBM25 Ab. β-Actin served as a loading control.

efficient utilization of the Bcl-x_S 5′ ss, resulting in an increased ratio of Bcl-x_S to Bcl-x_L. On the other hand, no effects on capase-3, Mcl1, and Fas were detected (Fig. 4A, casp-3, Mcl1, and Fas). Since the inclusions of the alternative exons in these transcripts are already vastly predominant, their response to RBM25 was then further evaluated in an RBM25 knockdown background (Fig. 4B). Treatment of cells with an RBM25 shRNA depleted the endogenous RBM25 by 85% (Fig. 4B, anti-RBM25, lanes non- and sh-82); nevertheless, no changes in the splicing pattern were detected. The alternative splicing of caspase-3, Mcl1, and Fas was not affected by RBM25 (Fig. 4B, casp-3, Mcl1, and Fas). Thus, the effect of RBM25 on Bcl-x pre-mRNA processing was specific and not attributable to a generalized effect on the RNA splicing machinery.

Increased RBM25 expression correlates with increased Bcl-x_S 5′ ss usage. To investigate the regulation of Bcl-x splicing by RBM25, we used a Bcl-x minigene (a gift from C. E. Chalfant, Virginia Commonwealth University, Richmond) that spans the entire alternatively spliced region from exon 1 to exon 3, with a shortened intron 2 (Fig. 5A). The Bcl-x minigene produced the same Bcl-x splicing pattern as seen with endogenous Bcl-x and produced two splice variants of the Bcl-x transcripts with a ratio of Bcl-x_S to Bcl-x_L of 0.31 in HeLa cells (Fig. 5B, lane 0). Cotransfection of pcDNA3.1-HA-RBM25 with this reporter activated splicing pathways which led to increased short variant Bcl-x_S with respect to transfection of pcDNA3.1-HA alone (Fig. 5B, lanes 0, 0.25, 0.5, 0.75, 1.00, and 1.50). The selection of the upstream 5′ ss in exon 2, resulting in

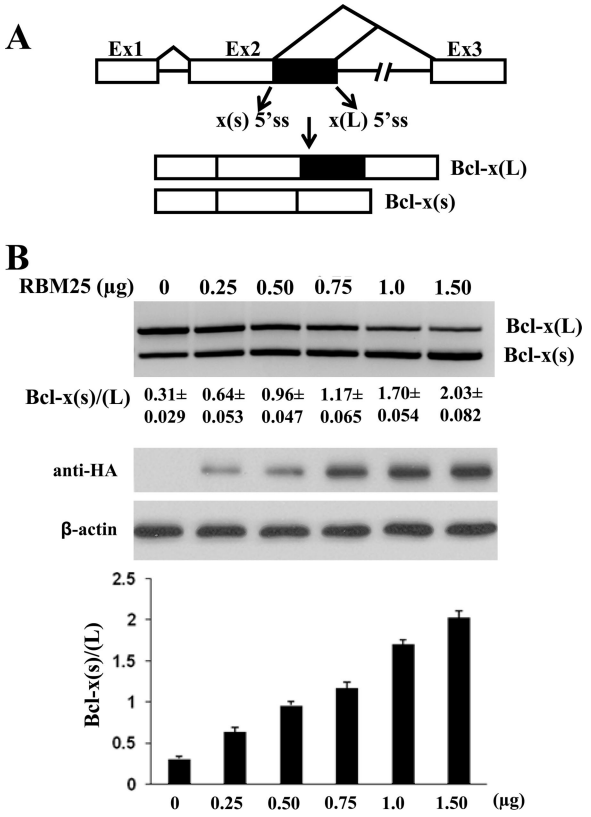

FIG. 5. RBM25 regulates Bcl-x 5′ ss selection. (A) Schematic diagram of the Bcl-x minigene spanning the entire alternatively spliced region from exon 1 to exon 3, with a shortened intron 2. Two splice variants derived from the Bcl-x gene, proapoptotic Bcl-x_S and antiapoptotic Bcl-x_L, are produced via alternative 5′ ss selection within exon 2. (B) Overexpression of RBM25 increased levels of proapoptotic Bcl-x_S in a dose-dependent manner. HeLa cells were transfected with 0.5 μg of Bcl-x minigene and increasing amounts of pcDNA3.1-HA-RBM25 (0 to 1.5 μg) and harvested 24 h after transfection. Semiquantitative RT-PCR was performed to determine the relative abundance of Bcl-x_S and Bcl-x_L mRNAs by densitometric analysis. Mean values ± SD of three independent experiments are shown. Anti-HA Western blotting indicates the expression levels of exogenous RBM25 proteins. β-Actin served as a loading control. The bar graph presents the densitometric analyses of the ratio of Bcl-x_S to Bcl-x_L from the three experiments performed (mean ± SD).

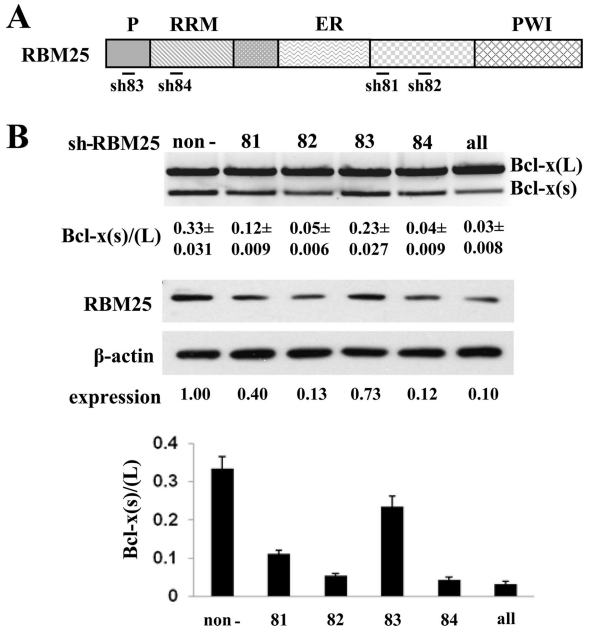

FIG. 6. Depletion of RBM25 by RNA interference leads to reduction of proapoptotic Bcl-x_S. (A) Schematic of RBM25 regions targeted by RBM25 shRNAs (sh81, sh82, sh83, and sh84). P, proline-rich region; RRM, RNA recognition motif; ER, glutamic acid/arginine-rich domain; PWI, proline-tryptophan-isoleucine domain. (B) HeLa cells were transfected with RBM25 shRNAs or nonsilencing controls. Semiquantitative RT-PCR was performed to determine alternatively spliced forms of Bcl-x 24 h after transfection. RBM25 expression levels in shRNA-treated cells relative to nonsilenced cells are shown at the bottom. Western blotting indicates the expression levels of endogenous RBM25 proteins. β-Actin served as a loading control. The bar graph presents the densitometric analyses of the ratio of Bcl-x_S to Bcl-x_L from the three experiments performed (mean ± SD).

the production of Bcl-x_S, was stimulated in an RBM25 dose-dependent manner (Fig. 5B). The addition of 0.25 μg RBM25 increased the ratio of Bcl-x_S to Bcl-x_L to 0.64, while the ratio increased to 2.3 when 1.5 μg of RBM25 was introduced. The expression of RBM25 was validated by a Western blot assay with anti-HA Abs (Fig. 5B, anti-HA). These results suggest that the Bcl-x reporter gene responded to RBM25 by enhancing Bcl-x_S 5′ ss usage.

Depletion of RBM25 reduces Bcl-x_S 5′ ss usage. The observation that increased expression of RBM25 could enhance the usage of the Bcl-x_S 5′ ss prompted us to examine whether reduction of RBM25 expression would block the usage of the same 5′ ss. Several RBM25 shRNA constructs (Fig. 6A), individually or in combination, reduced endogenous RBM25 expression in HeLa cells (Fig. 6B, RBM25, lanes sh81, sh82, sh83, sh84, and all). A nonfunctional control nonsilencing shRNA served as a control (Fig. 6B, RBM25, lane non).

We analyzed Bcl-x splicing patterns in RBM25 shRNA-treated cells. The nonsilencing control did not affect the splicing patterns (Fig. 6B, lane non) compared with that of untreated cells (Fig. 5B, lane 0). Reduction in RBM25 clearly affected the Bcl-x splicing pattern, in which a discernible decrease in Bcl-x_S 5′ ss usage was observed in RBM25 shRNA-treated cells (Fig. 6B, lanes non, sh81, sh82, sh83, sh84, and all). Bcl-x_S production was reduced by 3- to 10-fold. The decrease corresponded to the potency of the sh-RBM25 used to knock down RBM25 (Fig. 6B, expression, lanes non, sh81, sh82, sh83, sh84, and all). These results further suggest an involvement of RBM25 in the determination of 5′ ss selection in the Bcl-x gene.

RBM25 promotes Bcl-x_S 5′ ss usage through CGGGCA in exon 2. To examine whether RBM25 exerted its activity through an interaction with a *cis*-acting element, we first identified RNA sequences that have an effect on 5′ ss selection in response to RBM25 expression levels. We generated mutant forms of Bcl-x minigenes in which we replaced several sequences spanning exon 2 (Fig. 7A). Except for Mu1 and Mu5 (Fig. 7B, −RBM25, lanes Mu1 and Mu5), the replacements affected the splicing pattern with either increased (Fig. 7B, −RBM25, lane Mu2) or decreased ratios of Bcl-x_S to Bcl-x_L

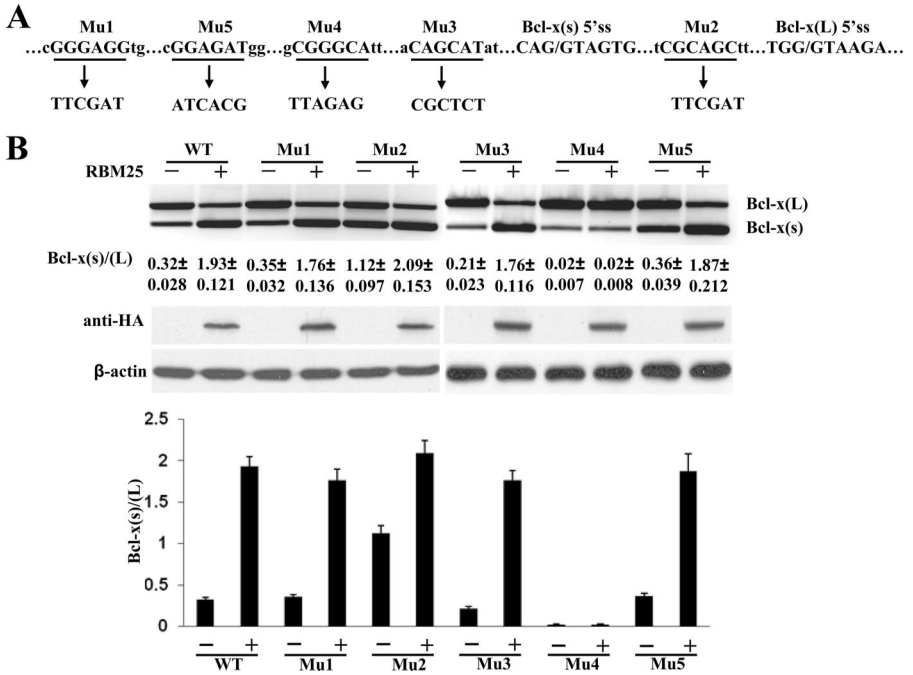

FIG. 7. A sequence motif within exon 2 is important for regulated splicing of Bcl-x by RBM25. (A) A diagram indicating mutated sequences and nucleotides replaced in the Bcl-x minigene tested in the experiment. (B) Analysis of the effect of mutations on Bcl-x splice site selections in response to RBM25. The minigene and its mutated constructs were transfected into HeLa cells either with a vector alone or with an RBM25-expressing plasmid and analyzed for the expression of Bcl-x isoforms. An anti-HA Ab was used to detect expression levels of transfected RBM25 proteins. β-Actin served as a loading control. The bar graph presents the densitometric analyses of the ratio of Bcl-x_S to Bcl-x_L in the three experiments performed (mean ± SD). −, no RBM25; +, with RBM25.

(Fig. 7B, −RBM25, lanes Mu3 and Mu4) compared with that of the WT (Fig. 7B, −RBM25, lane WT). These results suggest that the exonic sequences could activate or repress Bcl-x_S 5′ ss usage.

We then examined whether the mutated minigenes would still be responsive to RBM25 by cotransfection of RBM25 and the minigenes into HeLa cells. All but one responded to the stimulation of RBM25 by increasing the ratio of Bcl-x_S to Bcl-x_L (Fig. 7B, +RBM25, lanes WT, Mu1, Mu2, Mu3, and Mu5). Mutation of an element, CGGGCA, located 64 to 69 nt upstream of the Bcl-x_S 5′ ss drastically reduced Bcl-x_S expression and shifted the ratio of Bcl-x_S to Bcl-x_L from 0.33 to 0.02 (Fig. 7B, −RBM25, lane Mu4). Furthermore, mutation of this element abolished the ability of RBM25 to affect 5′ ss selection (Fig. 7B, +RBM25, lane Mu4). These results suggest that RBM25 might exert its activity through its binding to the CGGGCA element.

RBM25 associates with Bcl-x transcript and interacts with CGGGCA in vitro. We then investigated whether the endogenous Bcl-x RNA was associated with RBM25 by using an RIP assay with an anti-RBM25 Ab. RNA templates retrieved by RIP were analyzed by RT-PCR with primer sets to detect Bcl-x RNA. As shown in Fig. 8A, Bcl-x RNA was detected in both input and anti-RBM25 precipitates (Fig. 8A, input, α-RBM25, lanes +RT). The specificity of RNA IP is evidenced by the fact that IgG did not precipitate Bcl-x RNA (Fig. 8A, Bcl-x, IgG, lane +RT). Furthermore, no products were detected in the absence of RT (Fig. 8A, Bcl-x, α-RBM25, lane −RT). These results suggest that Bcl-x RNA associates with RBM25. To ensure that anti-RBM25 Ab did not pull down any nonspecific RNA sequences, we amplified isolated RNA for the presence of Mcl1 with its specific primer sets. While Mcl1 RNA was detected in the input, it was not found in anti-RBM25 precipitates (Fig. 8A, Mcl1, input and α-RBM25, lanes +RT). These results are consistent with the notion that Mcl1 is not a substrate of RBM25 and validate the specificity of the RIP assay.

To further examine whether RBM25 binds to CGGGCA directly, we performed an electrophoretic mobility shift analysis with CGGGCA-containing RNA and purified RBM25 protein. We examined the specific interaction between RBM25 and CGGGCA with a probe derived from the WT consisting of the sequences flanked by 6 nt upstream and 8 nt downstream (Fig. 8B, WT). The mutant sequence TTAGAG, flanked by identical upstream and downstream sequences (Fig. 8B, Mut), served as a control. The intensity of the retarded band increased when the WT probe was incubated with increasing amounts of RBM25 (Fig. 8C, WT, lanes 0, 0.5, 1.0, 2.0, and 4.0 μM). GST alone did not bind to the RNAs (Fig. 8C, WT, lane GST). No retarded bands were observed when increased amounts of RBM25 were incubated with the mutant probe (Fig. 8C, Mut, lanes 0, 0.5, 1.0, 2.0, and 4.0 μM). To assess the specificity of this WT RNA-protein interaction, a binding competition assay was performed with a 1-, 5-, or 20-fold molar excess of unlabeled WT or mutant RNA. The RNA-protein complexes were partially competed away by a 5-fold excess, and completely competed away by a 20-fold excess, of WT (Fig. 8D, WT) but not mutant RNA (Fig. 8D, Mut), suggesting that

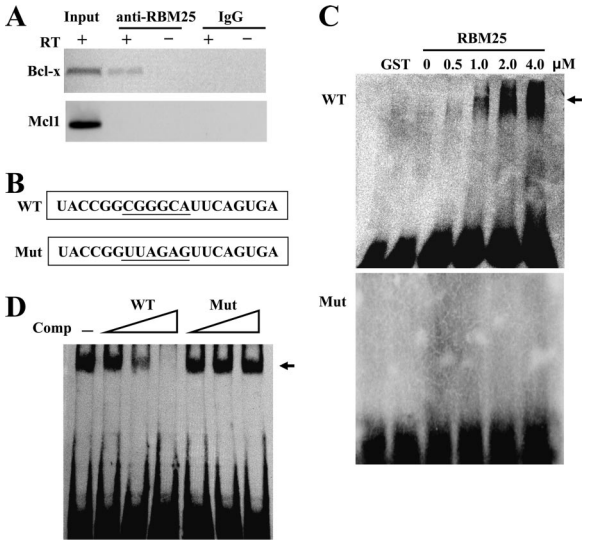

FIG. 8. RBM25 binds to Bcl-x RNA through the exonic sequence CGGGCA. (A) Bcl-x RNAs detected by RIP with an anti-RBM25 Ab. HeLa cells were fixed with 1% formaldehyde, and RIP was carried out with the cross-linked cell lysate and anti-RBM25 Ab or control rabbit IgG. PCR was performed with Bcl-x or Mcl1 primers on RNA retrieved by RIP with or without the RT reaction. The input lysate served as a positive control. (B) RNA probes consist of the WT or mutated (Mut) exonic sequences used in gel mobility shift assays. (C) Gel mobility shift assays were performed with the biotinylated WT or mutant probes and purified RBM25 proteins. Increasing amounts of RBM25 were incubated with the RNA probes, fractionated in a native 5% polyacrylamide gel, transferred to Hybond-N+ nylon membrane, and detected with a LightShift chemiluminescent electrophoretic mobility shift assay kit as described in Materials and Methods. Arrow, probe-protein complex. (D) For competition assay, a 1-, 5-, or 20-fold molar excess of unlabeled WT or mutant RNA was added to binding reaction mixtures. −, the probe incubated in the absence of competitors. Arrow, probe-protein complex.

the observed WT RNA-RBM25 interaction is CGGGCA sequence specific.

CGGGCA activates splicing from a weak 5′ ss in a test E1A reporter system. To pinpoint whether CGGGCA conferred RBM25 sensitivity, we examined the element in the context of the E1A reporter gene. A naturally occurring CGGGCA element is located 88 to 94 nt upstream of the 13S 5′ ss in E1A (Fig. 9A). Transfection of an E1A minigene alone produced three major classes of mRNAs with ~46% 13S, 38% 12S, and 16% 9S through the use of alternative 5′ ss (Fig. 9B, non, lane −RBM25). The 13S 5′ ss is much stronger than the 12S or 9S 5′ ss. Unexpectedly, the presence of cotransfected RBM25 did not change the overall splicing pattern (Fig. 9B, non, lane +RBM25). We then asked whether the effect of CGGGCA would be more potent in the context of a weak 9S 5′ ss. We created E1A+WT and E1A+Mu4 constructs in which the WT (UGGGCA) or the Mu4 (TTAGAG) sequence was inserted at positions 64 to 69 upstream of the 9S 5′ ss, respectively. The presence of UGGGCA resulted in a shift in splicing favoring the use of the 9S 5′ ss; an elevated 9S accounted for ~25% and a concomitant reduction of 12S to ~30% (Fig. 9B, WT, lane −RBM25). Cotransfection of RBM25 promoted ~25% more 9S splicing (Fig. 9B, WT, lane +RBM25). The insertion of Mu4 sequence exerted no significant effect on splicing in either the absence or the presence of RBM25 (Fig. 9B, Mu4, lanes −RBM25 and +RBM25). These results suggest that UGGGCA could enhance the utilization of the weak 9S 5′ ss but not that of a strong 13S 5′ ss through its interaction with RBM25.

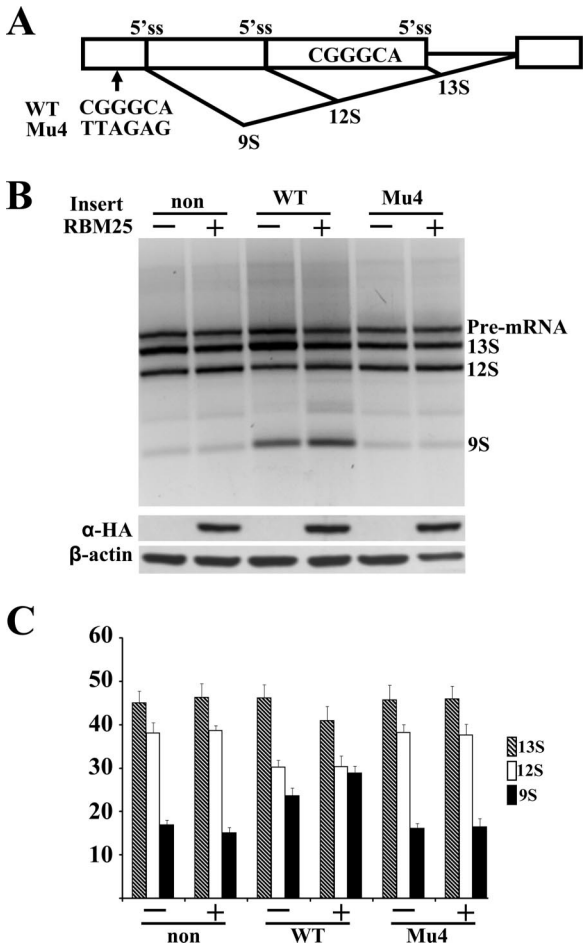

FIG. 9. Effect of CGGGCA on E1A reporter gene 5′ ss selection in vivo. (A) Schematic diagram of the E1A minigene and its major splicing products. E1A+WT and E1A+Mu4 constructs were created in which the WT (UGGGCA) or the Mu4 (TTAGAG) sequence was inserted at a position 64 to 69 nt upstream of the 9S 5′ ss, respectively. (B) In vivo splicing assays were performed with HeLa cells transfected with the E1A+non, E1A+WT, or E1A+Mu4 construct in the presence or absence of the expression vector pCDNA3.1-HA-RBM25. RNAs were isolated 24 h posttransfection and analyzed for E1A splicing products. Anti-HA Western blotting indicates the expression levels of exogenous RBM25 proteins. β-Actin served as a loading control. (C) The relative abundance of spliced mRNA species was analyzed by densitometric analysis. −, no RBM25; +, with RBM25. Mean values ± SD of three independent experiments are shown. The bar graph presents the densitometric analyses of the expression levels of 13S, 12S, and 9S from the three experiments performed (mean ± SD).

RBM25 facilitates the recruitment of U1 snRNP to the weak 5′ ss. The observation that CGGGCA exerted its effect on a weak 5′ ss prompted us to examine how RBM25 activated a 5′ ss with Bcl-x. We first analyzed the strength of Bcl-x 5′ ss with the Analyzer Splice Tool (http://ast.bioinfo.tau.ac.il/SpliceSiteFrame.htm), which uses an algorithm based on the work of Shapiro and Senapathy (45) to calculate the scores of donor and acceptor

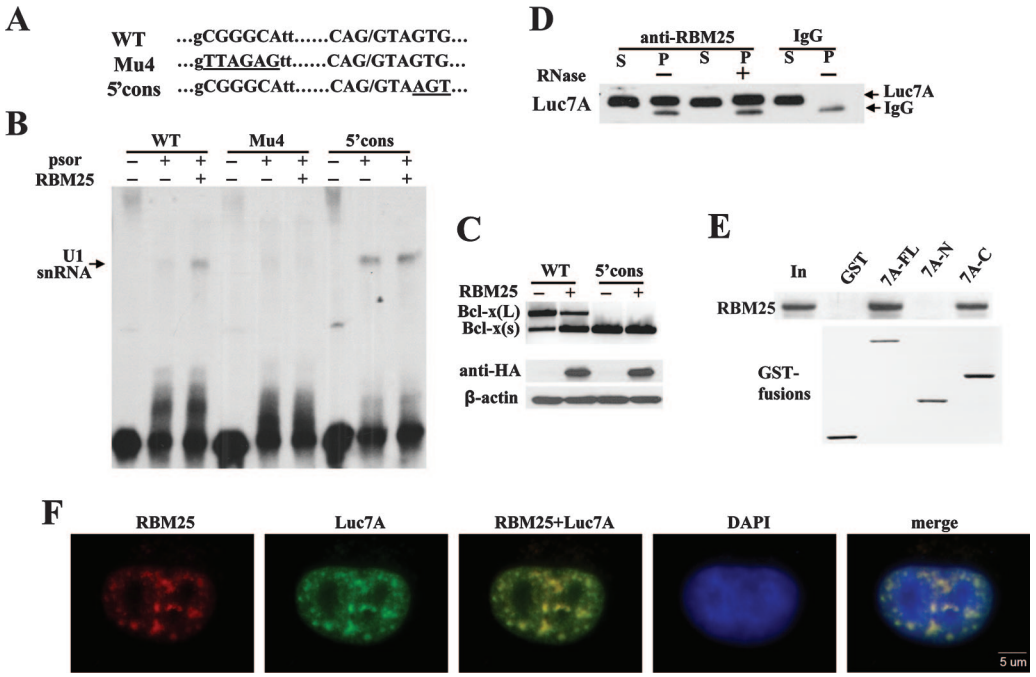

FIG. 10. RBM25 associates with hLuc7A and promotes U1 snRNP binding to a weak 5′ ss in a CGGGCA-dependent manner. (A) The WT, CGGGCA-to-TTAGAG mutant (Mu4), or consensus 5′ ss mutant (5′cons) Bcl-x minigene with the mutation sequence indicated in the diagram. (B) Weak 5′ ss is central in establishing CGGGCA-dependent recruitment of U1 snRNP by RBM25. Radioactively labeled Bcl-x_S substrates were incubated in HeLa cell nuclear extracts in the absence (−) or presence (+) of psoralen (psor), irradiated with 365-nm UV light, and fractionated on a denaturing polyacrylamide gel. Purified RBM25 was also added to the reaction mixtures as indicated. The position of the U1 snRNA/Bcl-x substrate cross-link is indicated. (C) Effect of RBM25 on WT or consensus Bcl-x_S 5′ ss (5′cons) minigene splicing. The minigenes were cotransfected with the empty vector or RBM25 cDNA into HeLa cells. Bcl-x isoforms were detected by RT-PCR. Anti-HA Ab was used to detect the expression levels of transfected RBM25 proteins. β-Actin served as a loading control. (D) Co-IP of RBM25 with hLuc7A by anti-RBM25 Ab. Western blot analysis of coimmunoprecipitated hLuc7A in the presence (+) or absence (−) of RNase. Preimmune rabbit IgG served as a control. S, IP supernatant; P, IP beads. (E) Association of RBM25 and hLuc7A analyzed in a GST pull-down assay. (Top) Pull-down assay of RBM25 with GST fusion proteins of full-length hLuc7A (7A-FL), its N-terminal half (7A-N), and its C-terminal half (7A-C). In, input lysates. (Bottom) Coomassie blue staining of purified GST-hLuc7A fusion proteins used in the experiment and separated by sodium dodecyl sulfate-polyacrylamide gel electrophoresis. (F) The localization of endogenous RBM25 and pCGT7-hLuc7A was detected with anti-RBM25 and anti-T7 Ab, respectively. Bar, 5 μm.

sequences. Bcl-x_S possesses a weak 5′ ss with a score of 72.66, while Bcl-x_L 5′ ss is relatively stronger at 81.51; the reference consensus sequence CAG/GTAAGT has a score of 100 (Fig. 10A).

Early recognition of the 5′ ss involves base-pairing interaction with the 5′ end of U1 snRNA. We performed psoralen-mediated UV cross-linking assays to examine whether U1 snRNP is recruited to transcripts containing the Bcl-x_S 5′ ss (Fig. 10B, WT). A psoralen-dependent cross-linked U1 snRNA/Bcl-x was detected upon incubation of a radioactively labeled WT sequences in HeLa cell nuclear extracts (Fig. 10B, WT, lane +/−). This interaction was significantly enhanced when ~300 ng of purified RBM25 was added (Fig. 10B, WT, lane +/+), suggesting that the presence of RBM25 facilitates U1 snRNP binding.

To determine whether the sequence CGGGCA is required for U1 interaction with the Bcl-x_S 5′ ss, we repeated the psoralen cross-linking assay with a Mut4 mutant probe. Mutations in the RBM25 binding site reduced the cross-linking product to a small extent (Fig. 10B, Mu4, lane +/−) compared with that of the WT probe (Fig. 10B, WT, lane +/−). In contrast to the WT probe, the addition of RBM25 did not promote U1 cross-linking to the Mu4 transcript (Fig. 10B, Mu4, lane +/+). These results suggest that RBM25-dependent U1 recruitment requires CGGGCA.

Data from Fig. 9B suggest that the presence of CGGGCA, followed by a strong 13S 5′ ss, had no effect on 13S splicing activity in the presence of RBM25. We thus tested whether an increased strength in Bcl-x_S 5′ ss would attenuate the effects of RBM25 in a cross-linking assay with Bcl-x_S and a consensus 5′ ss probe (Fig. 10A, 5′cons). The 5′cons transcripts cross-linked to U1 snRNA (Fig. 10B, 5′cons, lane +/−) much more strongly than did the WT in the absence of added RBM25 (Fig. 10B, WT, lane +/−). Addition of RBM25 did not increase 5′cons cross-linking to U1 snRNA (Fig. 10B, 5′cons, lane +/+). These data suggest that the contribution of RBM25 to U1 snRNP recruitment is particularly critical for a weak 5′ ss.

Subsequently, we analyzed the effect of the strength of Bcl-x_S 5′ ss on splicing and its response to RBM25 in HeLa cells. Strengthening Bcl-x_S 5′ ss to consensus sequence led to ~100% usage of the 5′ ss in the absence of RBM25 (Fig. 10C, 5′cons, lane −RBM25). Although RBM25 had an enhanced effect on the selection of the weak WT 5′ ss (Fig. 10C, WT, lane +RBM25), a strong 5′ ss did not require facilitation by RBM25 for the 5′ ss selection (Fig. 10C, 5′cons, lane +RBM25). These results suggest that RBM25 may facilitate

WT 5′ ss recognition by improving the interaction between U1 snRNA and the weak 5′ ss.

RBM25 associates with hLuc7A. Several positive regulators activate splicing of alternative exons with a weak 5′ ss by promoting interaction of U1 snRNP with the 5′ ss. U1 snRNP recognizes the 5′ ss and is among the first factors to interact with the pre-mRNA to form "complex E," which commits the pre-mRNA to the splicing pathway (26). We explored the possibility that RBM25 associates with the U1 snRNP complex and plays a role in recruiting U1 snRNP to the weak 5′ ss. U1 snRNP is composed of a 165-nt RNA (U1 snRNA), seven different Sm proteins common to other snRNP, and three U1-specific proteins (U1-70K, U1-A, and U1-C) (38). To probe the interactions between RBM25 and U1 snRNP, RBM25 was immunoprecipitated from HeLa cell nuclear extracts and analyzed by Western blotting for the presence of U1-specific proteins. No U1-specific proteins were detected in the precipitates (data not shown).

Human Luc7A has recently been shown to associate with U1-A and U1 snRNA and stabilize pre-mRNA–U1 snRNP interaction (36). We thus examined whether RBM25 associated with hLuc7A in the immunoprecipitates. Since RBM25 contains RRM and PWI motifs, both of which can bind to RNA, we also examined whether the association is RNA mediated. As shown in Fig. 10D, hLuc7A was abundantly detected in anti-RBM25 immunoprecipitates in an RNase-independent manner (Fig. 10D, α-RBM25, lane p, +RNase). The association of hLuc7A with RBM25 is most likely through the carboxyl half of hLuc7A because both the full length and the C half of hLuc7A, but not the N half, pulled down RBM25 in a GST pull-down experiment (Fig. 10E). Furthermore, hLuc7A colocalized in the nuclear speckles with RBM25 (Fig. 10F, RBM25+Luc7A). These results suggest that binding of RBM25 to the CGGGCA sequence may help recruitment of U1 snRNP to the weak 5′ ss through its interaction with U1 snRNP-associated hLuc7A and provide a molecular mechanism for the function of this splicing regulator.

DISCUSSION

The present study identifies a novel splicing factor, RBM25, which modulates apoptosis through regulation of Bcl-x isoform expression. RBM25 associates with a U1 snRNP-associated factor, hLuc7A, and activates Bcl-x_S 5′ ss via its interaction with the exonic splicing enhancer CGGGCA. Through both gain-of-function and loss-of-function experiments, we provide the first direct evidence that intracellular RBM25 levels affect the ratio of proapoptotic Bcl-x_S to antiapoptotic Bcl-x_L mRNA. Thus, we suggest that RBM25 is a member of a family of RNA-binding regulators that direct alternative splicing of apoptotic factor Bcl-x.

RBM25 has recently been proposed to regulate splicing; however, no direct pre-mRNA targets were identified (16). The correlation between RBM25 expression and the induction of apoptosis suggest that RBM25 either directly or indirectly targets proteins involved in apoptosis or apoptotic pathways. Here we show that regulation of apoptosis by RBM25 involves alternative splicing of its cellular target, Bcl-x. Bcl-x pre-mRNA employs alternative 5′ ss to produce the antiapoptotic Bcl-x_L or the proapoptotic Bcl-x_S isoforms (4). An increase in RBM25 has a significant effect in promoting the selection of the Bcl-x_S 5′ ss, whereas reduction of RBM25 shifts the balance toward the antiapoptotic Bcl-x_L) form.

Our results and those of others (16) showed that overexpression or depletion of RBM25 had no detectable in vivo effect on splicing of several tested endogenous genes. The effect of RBM25 in modulating the selection of Bcl-x_S 5′ ss seems to strictly depend on its specific interaction with an exonic element, CGGGCA, situated 64 to 69 nt upstream of the Bcl-x_S 5′ ss. Thus, we propose that RBM25 is a substrate-specific splicing regulator rather than an essential constitutive splicing factor. Database searches revealed that the sequence motif CGGGCA is present in many alternatively, as well as constitutively, spliced exons. Whether RBM25 exerts similar functional activity in the splicing of these exons is yet to be determined.

The contribution of RBM25 becomes negligible when CGGGCA is associated with a strong 13S 5′ ss in an E1A reporter or when base-pairing complementarity between Bcl-x_S 5′ ss and U1 snRNA is improved. Therefore, the necessity of RBM25 to activate the weak 5′ ss implies that binding to CGGGCA facilitates 5′ ss recognition by U1 snRNP. RBM25 has been shown to associate with U1 snRNAs (16). Our immunoprecipitation and GST-pull down results suggest that these associations are most likely not through the association of RBM25 with U1-specific proteins (U1A, U1C, or U1-70K) but via interactions with hLuc7A, the human homolog of yeast U1 snRNP component yLuc7p. RBM25-containing speckles are also precisely colocalized with hLuc7A nuclear structures, which further suggests cross talk between these proteins. Several lines of evidence support a role for Luc7 in splicing regulation in both yeast and mammalian cells. Yeast yLuc7p is required for commitment complex formation in vitro and is necessary for weak 5′ ss recognition by U1 snRNP (15). Mammalian hLuc7A is loosely associated with the human U1 snRNP and affects 5′ ss selection by stabilizing U1 snRNP-pre-mRNA interactions, as well as being involved in the formation of the E complex (36). Moreover, hLuc7A has recently been identified as a component of the supraspliceosome (9) and interacts with splicing factors RNPS1 (40) and SRrp53 (6).

Our identification of the association between hLuc7A and RBM25 provides insight into the mechanisms of RBM25 splicing activation. Binding of RBM25 to the exonic sequence CGGGCA could activate a weak 5′ ss through its interaction with hLuc7A, which directly binds to the U1 snRNP necessary for 5′ ss recognition. This activity would be reminiscent of TIA-1, which binds to U-rich sequences downstream of the weak 5′ ss and facilitates recruitment of U1 snRNP and production of the proapoptotic Fas receptor isoform (13). Future experiments are required to define in further detail the nature and chronology of the interactions among RBM25, hLuc7A, U1 snRNP, and the 5′ ss.

The molecular structure of RBM25 suggests that it contains domains essential for splicing regulation. The nuclear localization signal prediction program (http://cubic.bioc.columbia.edu/cgi/var/nair/resonline.pl) identifies three putative signals situated within the RRM domain (aa 233 to 238), RE/RD domain (aa 414 to 426), and PWI domain (aa 706 to 711). We found that each signal governs the nuclear localization of its individual domain. In addition, the RE/RD-rich domain is responsible

for the nuclear speckle localization of RBM25. It has been shown that replacement of the RS domain of SF2/ASF with an RE or RD domain also mediates proper nuclear speckle localization, albeit to a lesser extent (7). The repeats in RBM25 may thus serve as a targeting signal to nuclear speckles.

Our studies also show that RBM25 and SC35 coredistribute to the enlarged speckles upon inhibition of transcription. As with other splicing factors, RBM25 can lose its interchromatin granule cluster connections in transcriptionally active nuclei and localize to the enlarged unconnected speckle domains in transcriptionally inactive nuclei during states of transcription inhibition (5, 34).

The alternation of positive and negative charges of the amino acid residues (arginine-aspartates in RD and arginine-glutamates in RE) is reminiscent of phosphorylated RS (arginine-phosphorylated serine) domains. Thus, the RE/RD-rich domain may also mimic the structural and functional properties of a natural phosphorylated RS domain that mediates protein-protein interactions. It has been shown that stable protein interactions between SAFB1/SAFB2 with Sam68/T-STAR are mediated primarily by their RE-rich regions and play an important role in in vivo selection of splice sites (44). We demonstrate that the carboxyl half of hLuc7A consists of multiple RE and RS repeats that interact with RBM25 in an RNA-independent manner. Whether RE/RD repeats of RBM25 are responsible for such interactions remains to be determined.

Alternative splicing plays a fundamental role in the control of apoptosis. Several pre-mRNAs for cell death factors are alternatively spliced, yielding isoforms with opposing functions during programmed cell death (42). The regulation of Bcl-x alternative splicing is of critical importance to the apoptotic process and is highly pertinent to the progression of cancer. The expression of Bcl-x_L increases in a number of lymphomas (52), while Bcl-x_S is downregulated in many types of cancer cells. Several *cis* elements and *trans*-acting factors have been shown to regulate Bcl-x isoform expression. hnRNP F/H (17) and Sam68 (35) induce Bcl-x_S expression, whereas SAP155 (28) favors the selection of Bcl-x_L. Furthermore, Bcl-x splicing is coupled to signal transduction, since ceramide (8, 28) and protein kinase C (37) also affect splicing regulation. The ratio of the Bcl-x_S to the Bcl-x_L isoform will likely be dictated by the coordinated contribution of both *cis*- and *trans*-acting factors. Even though RBM25 is abundantly expressed in many of the cell types examined, its expression was found to be regulated during erythroid differentiation. As a result, regulated expression of RBM25 may play a critical role in mediating temporal and/or spatial splicing decisions of its target genes within the cell. Moreover, changes in the expression of any of these factors may influence how cells respond to apoptotic signals.

A growing family of RRM-containing proteins has been attributed to modulate apoptosis (50). In this report, we not only identified a new exonic splicing enhancer element for Bcl-x_S splicing but also uncovered an important splicing regulator, RBM25, which interacts with this exonic splicing enhancer element to enhance the weak 5′ ss selection, most likely through its interaction with a U1 snRNP-associated protein, hLuc7A. We suggest that RBM25 is an RNA-binding apoptosis regulator. The mechanism of alternative 5′ ss selection of Bcl-x pre-mRNA has emerged as a potential target for anticancer therapeutics (51). Our studies will lead to greater insights into the molecular mechanisms by which RBM25 acts as a modulator of apoptosis.

ACKNOWLEDGMENTS

We thank O. Puig (European Molecular Biology Laboratory, Germany) for the hLuc7A plasmid, C. E. Chalfant (Virginia Commonwealth University, Richmond) for the Bcl-x minigene, and W. Y. Tarn (Institute of Biomedical Sciences, Academia Sinica, Taipei, Taiwan) for the E1A minigene. We thank H. R. Widlund (Dana-Farber Cancer Institute, Boston, MA) for valuable suggestions throughout this project.

This work was supported by a Claudia Barr Award (S.C.H.) and NIH grant HL24385 (E.J.B.).

REFERENCES

1. **Bingle, C. D., R. W. Craig, B. M. Swales, V. Singleton, P. Zhou, and M. K. Whyte.** 2000. Exon skipping in Mcl-1 results in a bcl-2 homology domain 3 only gene product that promotes cell death. J. Biol. Chem. **275:**22136–22146.
2. **Black, D. L.** 2003. Mechanisms of alternative pre-messenger RNA splicing. Annu. Rev. Biochem. **72:**291–336.
3. **Blencowe, B. J.** 2000. Exonic splicing enhancers: mechanism of action, diversity and role in human genetic diseases. Trends Biochem. Sci. **25:**106–110.
4. **Boise, L. H., M. Gonzalez-Garcia, C. E. Postema, L. Ding, T. Lindsten, L. A. Turka, X. Mao, G. Nunez, and C. B. Thompson.** 1993. bcl-x, a bcl-2-related gene that functions as a dominant regulator of apoptotic cell death. Cell **74:**597–608.
5. **Bregman, D. B., L. Du, S. van der Zee, and S. L. Warren.** 1995. Transcription-dependent redistribution of the large subunit of RNA polymerase II to discrete nuclear domains. J. Cell Biol. **129:**287–298.
6. **Cazalla, D., K. Newton, and J. F. Caceres.** 2005. A novel SR-related protein is required for the second step of pre-mRNA splicing. Mol. Cell. Biol. **25:**2969–2980.
7. **Cazalla, D., J. Zhu, L. Manche, E. Huber, A. R. Krainer, and J. F. Caceres.** 2002. Nuclear export and retention signals in the RS domain of SR proteins. Mol. Cell. Biol. **22:**6871–6882.
8. **Chalfant, C. E., K. Rathman, R. L. Pinkerman, R. E. Wood, L. M. Obeid, B. Ogretmen, and Y. A. Hannun.** 2002. *De novo* ceramide regulates the alternative splicing of caspase 9 and Bcl-x in A549 lung adenocarcinoma cells. Dependence on protein phosphatase-1. J. Biol. Chem. **277:**12587–12595.
9. **Chen, Y. I., R. E. Moore, H. Y. Ge, M. K. Young, T. D. Lee, and S. W. Stevens.** 2007. Proteomic analysis of in vivo-assembled pre-mRNA splicing complexes expands the catalog of participating factors. Nucleic Acids Res. **35:**3928–3944.
10. **Del Gatto-Konczak, F., C. F. Bourgeois, C. Le Guiner, L. Kister, M. C. Gesnel, J. Stevenin, and R. Breathnach.** 2000. The RNA-binding protein TIA-1 is a novel mammalian splicing regulator acting through intron sequences adjacent to a 5′ splice site. Mol. Cell. Biol. **20:**6287–6299.
11. **Del Gatto-Konczak, F., M. Olive, M. C. Gesnel, and R. Breathnach.** 1999. hnRNP A1 recruited to an exon in vivo can function as an exon splicing silencer. Mol. Cell. Biol. **19:**251–260.
12. **Dignam, J. D., R. M. Lebovitz, and R. G. Roeder.** 1983. Accurate transcription initiation by RNA polymerase II in a soluble extract from isolated mammalian nuclei. Nucleic Acids Res. **11:**1475–1489.
13. **Förch, P., O. Puig, N. Kedersha, C. Martinez, S. Granneman, B. Seraphin, P. Anderson, and J. Valcarcel.** 2000. The apoptosis-promoting factor TIA-1 is a regulator of alternative pre-mRNA splicing. Mol. Cell **6:**1089–1098.
14. **Förch, P., O. Puig, C. Martinez, B. Seraphin, and J. Valcarcel.** 2002. The splicing regulator TIA-1 interacts with U1-C to promote U1 snRNP recruitment to 5′ splice sites. EMBO J. **21:**6882–6892.
15. **Fortes, P., D. Bilbao-Cortes, M. Fornerod, G. Rigaut, W. Raymond, B. Seraphin, and I. W. Mattaj.** 1999. Luc7p, a novel yeast U1 snRNP protein with a role in 5′ splice site recognition. Genes Dev. **13:**2425–2438.
16. **Fortes, P., D. Longman, S. McCracken, J. Y. Ip, R. Poot, I. W. Mattaj, J. F. Caceres, and B. J. Blencowe.** 2007. Identification and characterization of RED120: a conserved PWI domain protein with links to splicing and 3′-end formation. FEBS Lett. **581:**3087–3097.
17. **Garneau, D., T. Revil, J. F. Fisette, and B. Chabot.** 2005. Heterogeneous nuclear ribonucleoprotein F/H proteins modulate the alternative splicing of the apoptotic mediator Bcl-x. J. Biol. Chem. **280:**22641–22650.
18. **Graveley, B. R., and T. Maniatis.** 1998. Arginine/serine-rich domains of SR proteins can function as activators of pre-mRNA splicing. Mol. Cell **1:**765–771.
19. **Hartmann, A. M., O. Nayler, F. W. Schwaiger, A. Obermeier, and S. Stamm.** 1999. The interaction and colocalization of Sam68 with the splicing-associated factor YT521-B in nuclear dots is regulated by the Src family kinase $p59^{fyn}$. Mol. Biol. Cell **10:**3909–3926.
20. **Hiller, M., Z. Zhang, R. Backofen, and S. Stamm.** 2007. Pre-mRNA secondary structures influence exon recognition. PLoS Genet. **3:**e204.

21. **Horowitz, D. S., and A. R. Krainer.** 1994. Mechanisms for selecting 5′ splice sites in mammalian pre-mRNA splicing. Trends Genet. **10:**100–106.
22. **Huang, Y., N. H. Shin, Y. Sun, and K. K. Wang.** 2001. Molecular cloning and characterization of a novel caspase-3 variant that attenuates apoptosis induced by proteasome inhibition. Biochem. Biophys. Res. Commun. **283:**762–769.
23. **Jurica, M. S., and M. J. Moore.** 2003. Pre-mRNA splicing: awash in a sea of proteins. Mol. Cell **12:**5–14.
24. **Kang, J., M. S. Lee, S. J. Watowich, and D. G. Gorenstein.** 2006. Chemiluminescence-based electrophoretic mobility shift assay of RNA-protein interactions: application to binding of viral capsid proteins to RNA. J. Virol. Methods **131:**155–159.
25. **Lopez, A. J.** 1998. Alternative splicing of pre-mRNA: developmental consequences and mechanisms of regulation. Annu. Rev. Genet. **32:**279–305.
26. **Maniatis, T., and B. Tasic.** 2002. Alternative pre-mRNA splicing and proteome expansion in metazoans. Nature **418:**236–243.
27. **Maris, C., C. Dominguez, and F. H. Allain.** 2005. The RNA recognition motif, a plastic RNA-binding platform to regulate post-transcriptional gene expression. FEBS J. **272:**2118–2131.
28. **Massiello, A., J. R. Roesser, and C. E. Chalfant.** 2006. SAP155 Binds to ceramide-responsive RNA cis-element 1 and regulates the alternative 5′ splice site selection of Bcl-x pre-mRNA. FASEB J. **20:**1680–1682.
29. **Matlin, A. J., F. Clark, and C. W. Smith.** 2005. Understanding alternative splicing: towards a cellular code. Nat. Rev. Mol. Cell Biol. **6:**386–398.
30. **Misteli, T., J. F. Caceres, and D. L. Spector.** 1997. The dynamics of a pre-mRNA splicing factor in living cells. Nature **387:**523–527.
31. **Nilsen, T. W.** 2002. The spliceosome: no assembly required? Mol. Cell **9:**8–9.
32. **Niranjanakumari, S., E. Lasda, R. Brazas, and M. A. Garcia-Blanco.** 2002. Reversible cross-linking combined with immunoprecipitation to study RNA-protein interactions in vivo. Methods **26:**182–190.
33. **Norton, P. A.** 1994. Alternative pre-mRNA splicing: factors involved in splice site selection. J. Cell Sci. **107:**1–7.
34. **O'Keefe, R. T., A. Mayeda, C. L. Sadowski, A. R. Krainer, and D. L. Spector.** 1994. Disruption of pre-mRNA splicing in vivo results in reorganization of splicing factors. J. Cell Biol. **124:**249–260.
35. **Paronetto, M. P., T. Achsel, A. Massiello, C. E. Chalfant, and C. Sette.** 2007. The RNA-binding protein Sam68 modulates the alternative splicing of Bcl-x. J. Cell Biol. **176:**929–939.
36. **Puig, O., E. Bragado-Nilsson, T. Koski, and B. Seraphin.** 2007. The U1 snRNP-associated factor Luc7p affects 5′ splice site selection in yeast and human. Nucleic Acids Res. **35:**5874–5885.
37. **Revil, T., J. Toutant, L. Shkreta, D. Garneau, P. Cloutier, and B. Chabot.** 2007. Protein kinase C-dependent control of Bcl-x alternative splicing. Mol. Cell. Biol. **27:**8431–8441.
38. **Rinke, J., B. Appel, H. Blocker, R. Frank, and R. Luhrmann.** 1984. The 5′-terminal sequence of U1 RNA complementary to the consensus 5′ splice site of hnRNA is single-stranded in intact U1 snRNP particles. Nucleic Acids Res. **12:**4111–4126.
39. **Ryan, K. J., B. N. Charlet, and T. A. Cooper.** 2000. Binding of PurH to a muscle-specific splicing enhancer functionally correlates with exon inclusion in vivo. J. Biol. Chem. **275:**20618–20626.
40. **Sakashita, E., S. Tatsumi, D. Werner, H. Endo, and A. Mayeda.** 2004. Human RNPS1 and its associated factors: a versatile alternative pre-mRNA splicing regulator in vivo. Mol. Cell. Biol. **24:**1174–1187.
41. **Sanford, J. R., J. Ellis, and J. F. Caceres.** 2005. Multiple roles of arginine/serine-rich splicing factors in RNA processing. Biochem. Soc. Trans. **33:**443–446.
42. **Schwerk, C., and K. Schulze-Osthoff.** 2005. Regulation of apoptosis by alternative pre-mRNA splicing. Mol. Cell **19:**1–13.
43. **Selvakumar, M., and D. M. Helfman.** 1999. Exonic splicing enhancers contribute to the use of both 3′ and 5′ splice site usage of rat beta-tropomyosin pre-mRNA. RNA **5:**378–394.
44. **Sergeant, K. A., C. F. Bourgeois, C. Dalgliesh, J. P. Venables, J. Stevenin, and D. J. Elliott.** 2007. Alternative RNA splicing complexes containing the scaffold attachment factor SAFB2. J. Cell Sci. **120:**309–319.
45. **Shapiro, M. B., and P. Senapathy.** 1986. Automated preparation of DNA sequences for publication. Nucleic Acids Res. **14:**65–73.
46. **Singh, R., and J. Valcarcel.** 2005. Building specificity with nonspecific RNA-binding proteins. Nat. Struct. Mol. Biol. **12:**645–653.
47. **Smith, C. W., and J. Valcarcel.** 2000. Alternative pre-mRNA splicing: the logic of combinatorial control. Trends Biochem. Sci. **25:**381–388.
48. **Spector, D. L., W. H. Schrier, and H. Busch.** 1983. Immunoelectron microscopic localization of snRNPs. Biol. Cell **49:**1–10.
49. **Stetefeld, J., and M. A. Ruegg.** 2005. Structural and functional diversity generated by alternative mRNA splicing. Trends Biochem. Sci. **30:**515–521.
50. **Sutherland, L. C., N. D. Rintala-Maki, R. D. White, and C. D. Morin.** 2005. RNA binding motif (RBM) proteins: a novel family of apoptosis modulators? J. Cell. Biochem. **94:**5–24.
51. **Taylor, J. K., Q. Q. Zhang, J. R. Wyatt, and N. M. Dean.** 1999. Induction of endogenous Bcl-xS through the control of Bcl-x pre-mRNA splicing by antisense oligonucleotides. Nat. Biotechnol. **17:**1097–1100.
52. **Xerri, L., P. Parc, P. Brousset, D. Schlaifer, J. Hassoun, J. C. Reed, S. Krajewski, and D. Birnbaum.** 1996. Predominant expression of the long isoform of Bcl-x (Bcl-xL) in human lymphomas. Br. J. Haematol. **92:**900–906.
53. **Yang, G., S. C. Huang, J. Y. Wu, and E. J. Benz, Jr.** 2005. An erythroid differentiation-specific splicing switch in protein 4.1R mediated by the interaction of SF2/ASF with an exonic splicing enhancer. Blood **105:**2146–2153.
54. **Yang, G., S. C. Huang, J. Y. Wu, and E. J. Benz, Jr.** 2008. Regulated Fox-2 isoform expression mediates protein 4.1R splicing during erythroid differentiation. Blood **111:**392–401.
55. **Zhou, H. L., A. P. Baraniak, and H. Lou.** 2007. Role for Fox-1/Fox-2 in mediating the neuronal pathway of calcitonin/calcitonin gene-related peptide alternative RNA processing. Mol. Cell. Biol. **27:**830–841.
56. **Zhu, H., R. A. Hasman, K. M. Young, N. L. Kedersha, and H. Lou.** 2003. U1 snRNP-dependent function of TIAR in the regulation of alternative RNA processing of the human calcitonin/CGRP pre-mRNA. Mol. Cell. Biol. **23:**5959–5971.
57. **Zhu, J., A. Mayeda, and A. R. Krainer.** 2001. Exon identity established through differential antagonism between exonic splicing silencer-bound hnRNP A1 and enhancer-bound SR proteins. Mol. Cell **8:**1351–1361.